Report CLRP 12–02

Data for an accurate transmission measurement benchmark

E. S. M. Ali[1], M. R. McEwen [2] and D. W. O. Rogers [1]
[1] Carleton Laboratory for Radiotherapy Physics,
Department of Physics, Carleton University.
1125 Colonel By Drive, Ottawa, ON K1S 5B6, Canada
[2] Ionizing Radiation Standards, Institute for National Measurement Standards,
National Research Council, M-35 Montreal Rd, Ottawa, ON K1A 0R5, Canada
E-mail: eali@physics.carleton.ca
malcolm.mcewen@nrc-cnrc.gc.ca
drogers@physics.carleton.ca

Available at: `http://www.physics.carleton.ca/clrp/transmission`

June 25, 2012

Abstract

This report supplements the primary benchmark publication: Ali *et al* "Detailed high-accuracy megavoltage transmission measurements: A sensitive experimental benchmark of EGSnrc", Med. Phys. **39**, xxxx – xxxx, (2012). The report provides the details needed to create a model of the transmission measurement setup for the purpose of benchmarking Monte Carlo codes. The experimental signals and the corresponding `EGSnrc` data are given in tabular form for the MV beams and bremsstrahlung targets that are included in the publication.

1 Introduction

In a recent study (Ali *et al* 2012), detailed high-accuracy megavoltage transmission measurements are performed using the research linac of the National Research Council (NRC) Canada. The incident electron parameters are independently known, and the measurement geometry is known and simple. This makes the resulting experimental transmission signals a useful primary benchmark of Monte Carlo codes. In the publication, the experimental setup is modelled using `EGSnrc` (Kawrakow 2000; Kawrakow *et al* 2011) and the `EGSnrc`-calculated transmission data are compared with the experimental signals.

This report provides the data needed to create a model of the transmission measurement setup for others to benchmark their Monte Carlo codes. The details are the incident electron beam parameters (§2), and the setup materials and dimensions (§3). The setup includes the targets, attenuators, collimators and detectors. The experimental signals and the corresponding `EGSnrc` data are given in tabular form for the MV beams and bremsstrahlung targets that are included in the publication (§4).

2 Incident electron beam parameters

Table 1: Incident electron parameters at the linac exit window.

Parameter	Description
Nominal MV	10, 15, 15.7, 20, 30 MV.
Mean energy	10.09, 15.00, 15.70, 20.28 and 30.00 MeV.
Energy spread	Gaussian, 0.4% standard deviation.
Focal spot	Gaussian, 1 mm FWHM.
Angular divergence	0.03°, virtual apex upstream at 1 m

3 Setup materials and dimensions

Figure 1 shows a schematic of the setup. It has symbols that are used in the tables of this report to give the setup details. In figure 1, the two axes are called x and y, rather than the more common r and z, because the Farmer chamber is irradiated side-on, and the same two axes are used to give the buildup cap dimensions in figure 3, therefore using r and z would be confusing.

Table 2 gives the materials of different geometric regions and their elemental composition. The surrounding medium is air, and its composition (as used in the `EGSnrc` calculations) is given.

The setup dimensions are given in table 3. Target thicknesses are presented separately in table 4 because they vary with the MV of the beam and with the target material. The successive attenuators lengths are given in table 5. Each length is identified by an index throughout the report. For a given MV beam and a given attenuator, the attenuator lengths used with the W-alloy cap are those with indices 2, 4, 6, 8 and 10, while those with indices 1, 3, 5, 7 and 9 are used with the PMMA (or the Al) cap.

The monitor chamber used is a PTW7862. It is modelled according to its drawing in the publicly available PTW catalog (2008 – 2009 version used). Briefly, the chamber consists of four Kapton foils, 50 μm-thick each, two of which are coated with graphite of negligible thickness. Its sensitive volume is a central air cylinder of diameter 9.65 cm and thickness 2.4 mm. The details of the model are shown in figure 2 and tables 2 and 3.

Two Farmer chambers are used: an Exradin A19 and a PTW30013. The dimensions of the in-house buildup caps that are used with the Farmer chambers are given in figure 3 and table 6. The material composition of the buildup caps used is given with the rest of the material definitions in table 2. The PTW30013 chamber is modelled according to its drawing in the PTW catalog mentioned above. The Exradin A19 is modelled from its blueprints, obtained through a Non-Disclosure Agreement (NDA). The interested reader can arrange for an NDA to model the chamber. Figure 4 shows an example of the chamber model in the `EGSnrc` simulations.

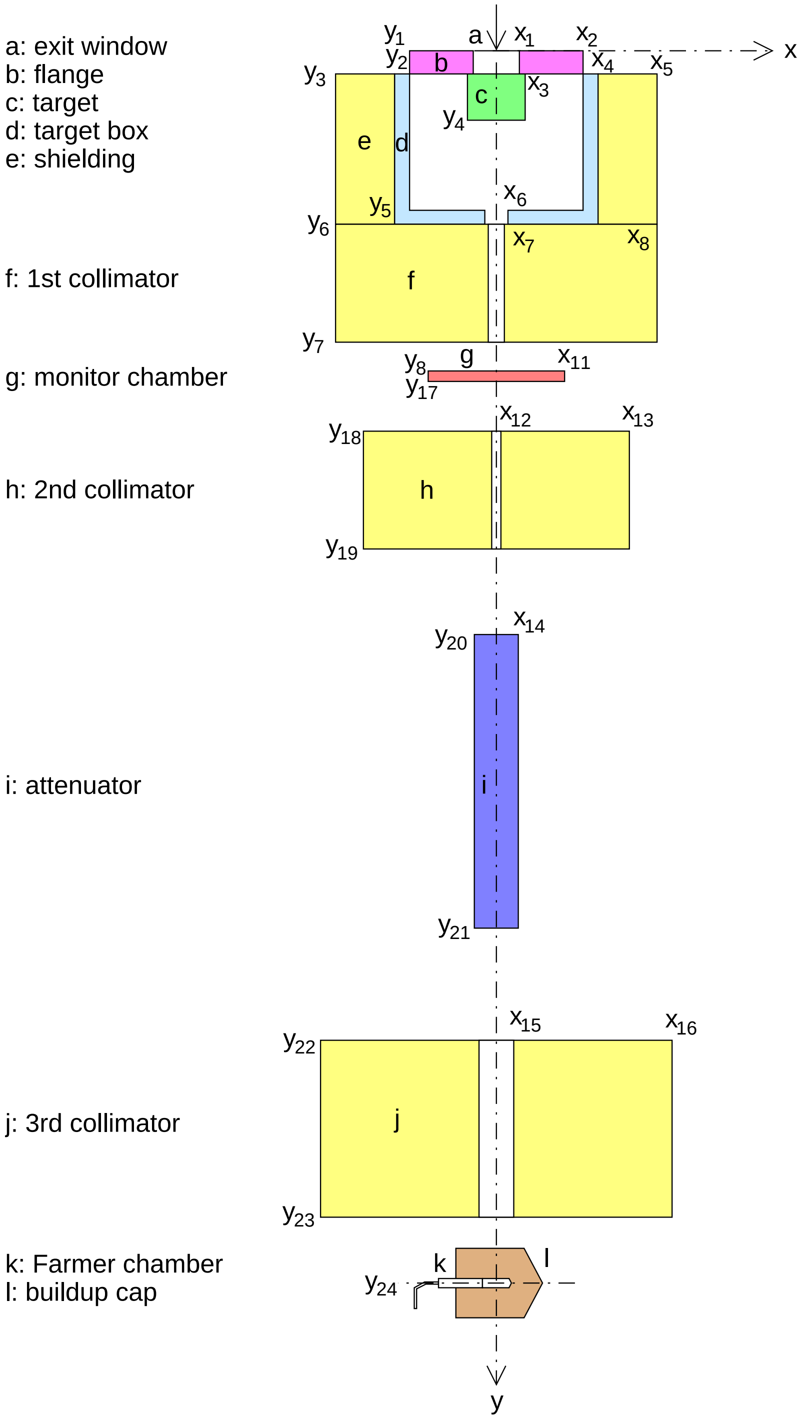

Figure 1: A schematic diagram of the transmission measurement setup (not to scale). The letters a to l are indices for the different geometric regions, and they are used in table 2 when listing the material composition of each region. The symbols x_i (where $i = 1 - 16$) and the y_i (where $i = 1 - 24$) represent dimensions that are given in tables 3, 4 and 5. An x_i dimension represents the radius if the geometric region has a circular cross section, and represents the half of the side length if the region has a square cross section. A y_i dimension is the distance from the upstream surface of the linac exit window. For the monitor chamber, what's shown are only the external dimensions (i.e., x_{11}, y_8 and y_{17}), whereas figure 2 shows its full dimensions (i.e., x_9 to x_{11} and y_8 to y_{17}).

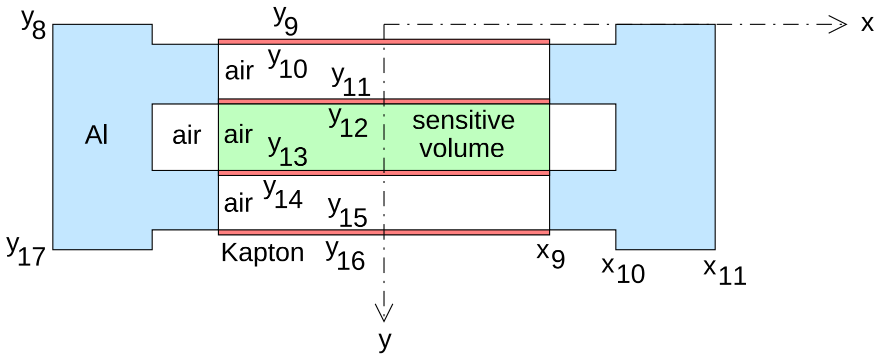

Figure 2: A schematic diagram of the monitor chamber (not to scale). The x and y axes are the same as those in figure 1. The external dimensions of the monitor chamber (i.e., x_{11}, y_8 and y_{17}) are the same as those shown in figure 1. The symbols x_i (where $i = 9 - 11$) and the y_i (where $i = 8 - 17$) represent dimensions that are given in table 3. The monitor chamber is geometric region g, and the material composition of its components are given in table 2.

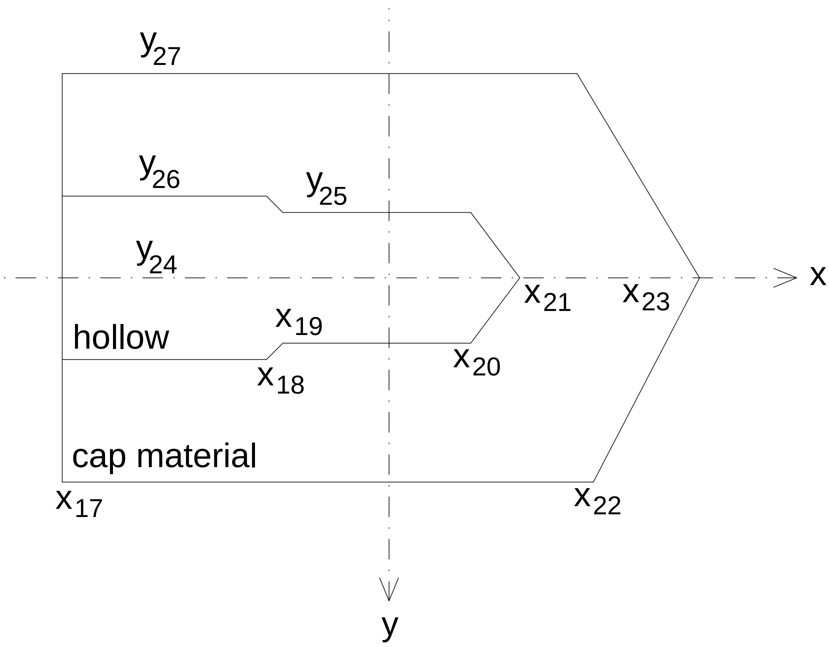

Figure 3: A schematic diagram of the buildup caps used with the Farmer chambers (not to scale). The Farmer chamber fits in the hollow part of the cap. The x and y axes are the same as those in figure 1, which means that the chamber (fitted with the buildup cap) is irradiated side-on. The location of the centerline of the cap downstream of the linac exit window is shown as y_{24}, which is the same as the y_{24} of figure 1. The symbols x_i (where $i = 17 - 23$) and the y_i (where $i = 25 - 27$) represent dimensions that are given in table 6. The cap is geometric region l, and its material composition is given in table 2 for the three caps used.

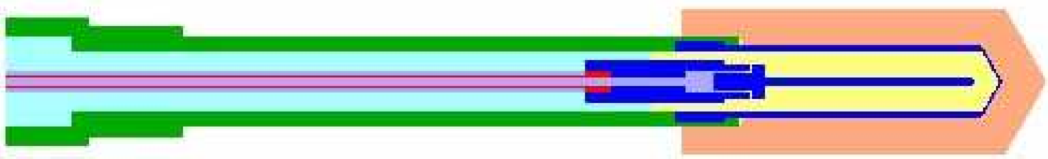

Figure 4: An example of the detector model used in the simulation. The figure shows the egs++ model (Muir and Rogers 2010) of the Exradin A19 Farmer chamber (from blueprints) fitted with the Hevimet buildup cap.

Table 2: Elemental composition of the materials of the different geometric regions in the setup. Each region is identified by an index, *a* to *l*, which is shown in figure 1.

Index	Region name	Name of material	Density g/cm^3	Elemental composition 'element symbol: weight fraction'
a	Exit window	Ti alloy	4.42	Ti: 0.90, Al: 0.06, V: 0.04
b	Flange	Steel 302	8.06	C: 0.001, Si: 0.007, Cr: 0.180, Mn: 0.010, Fe: 0.712, Ni: 0.090
c	Target	Be	1.848	Assumed pure
		Al	2.699	Assumed pure
		Be	11.35	Assumed pure
d	Target box	Al	2.699	Assumed pure
e	Shielding	Pb	11.35	Assumed pure
f	1st collimator	Pb	11.35	Assumed pure
g	Monitor	Al frame	2.699	Assumed pure
		Kapton	1.42	H: 0.026362, C: 0.691133, N: 0.073270, O: 0.209235
h	2nd collimator	Pb	11.35	Assumed pure
i	Attenuator	C bars	1.728	C: 0.999500. Impurities are: O: 0.000243, Na: 0.000004, Mg: 0.000015, Al: 0.000070, Si: 0.000128, P: 0.000002, K: 0.000004, Ca: 0.000011, Ti: 0.000006, Fe: 0.000017
		Pb rods	11.290	Pb: 0.999780. Impurities are: Mg: 0.000001, Ti: 0.000005, Fe: 0.000002, Cu: 0.000020, Ag: 0.000020, Cd: 0.000002, Sn: 0.000070, Bi: 0.000100
j	3rd collimator	Pb	11.35	Assumed pure
k	Farmer	–	–	See §3 for details
l	Buildup cap	Hevimet	16.88	Ni: 0.05, Cu: 0.05, W: 0.90
		PMMA	1.18	H: 0.0805380, C: 0.599848, O: 0.319614
		Al	2.699	Assumed pure
–	Surrounding	Air	0.0012048	C: 0.000124, N: 0.755267, O: 0.231781, Ar: 0.012827

Table 3: The x_i and the y_i setup dimensions shown in figures 1 and 2. An x_i dimension represents the radius if the geometric region has a circular cross section (denoted by *cir*), and represents the half of the side length if the region has a square cross section (denoted by *sq*). A y_i dimension is the distance from the upstream surface of the linac exit window. The target and attenuator dimensions are variable, and the rest of their information are given in tables 4 and 5, respectively.

i in x_i	Dimension in cm, *sq* or *cir*	i in y_i	Dimension in cm
1	1.9, *cir*	1	0.0
2	7.5, *cir*	2	0.00412
3	3.63, *cir* / 1.5, *sq*†	3	2.1
4	8.77, *sq*	4	See table 4
5	13.85, *sq*	5	13.7
6	1.0, *cir*	6	15.0
7	0.693, *cir*	7	25.2
8	13.85, *sq*	8	27.6
9	4.825, *cir*	9	27.695
10	5.075, *cir*	10	27.700
11	5.975, *cir*	11	27.925
12	0.387, *cir*	12	27.930
13	11.5, *sq*	13	28.170
14	1.905, *sq* / 0.950, *cir*‡	14	28.175
15	1.463, *cir*	15	28.400
16	15.2, *sq*	16	28.405
		17	28.500
		18	55.1
		19	65.3
		20	95.1
		21	See table 5
		22	276.5
		23	291.8
		24	298.8

† The '3.63, *cir*' is for the Be and Al targets, while the '1.5, *sq*' is for the Pb targets

‡ The '1.905, *sq*' is for the C attenuators, while the '0.950, *cir*' is for the Pb attenuators.

Table 4: Thicknesses of the bremsstrahlung targets used. The thicknesses should be added to y_3 in table 3 to give y_4.

Target material	Target thickness in cm 10 MV	15/15.7 MV	20 MV	30 MV
Be	–	6.31	–	–
Al	2.40	3.60	4.31	6.60
Pb	–	0.793	1.016	–

Table 5: Lengths of the attenuators for various beams. The lengths should be added to y_{20} in table 3 to give y_{21}. For C attenuators, the lengths given are already corrected such that when used with the average measured density from table 2 (i.e. 1.728 g/cm^3), the individual mass thickness of each bar is properly used in the simulation. For Pb attenuators, the lengths given are the physical lengths, and they are used with the average measured density from table 2 (i.e., 11.290 g/cm^3). Note that for Pb attenuators and a given transmission value, higher-MV beams require shorter lengths because the Pb attenuation coefficient has a minimum at $\sim$ 2.5 MeV.

	C attenuator lengths in cm			Pb attenuator lengths in cm		
Index	10 MV	15, 15.7 MV	20, 30 MV	10, 15, 15.7 MV	20 MV	30 MV
1	8.32	9.36	11.61	0.75	0.70	0.65
2	16.64	18.88	23.25	1.51	1.40	1.31
3	24.95	28.56	34.87	2.25	2.10	1.95
4	33.24	37.89	46.60	3.01	2.79	2.61
5	41.56	47.56	58.18	3.75	3.50	3.25
6	49.36	56.66	69.40	4.50	4.25	3.91
7	57.90	66.65	81.11	5.25	4.89	4.56
8	66.77	76.30	92.74	5.99	5.60	5.20
9	74.53	85.27	104.15	6.74	6.29	5.86
10	83.13	95.31	115.62	7.51	7.00	6.51

Table 6: Dimensions of the three buildup caps used with the Farmer chambers. The x_i and the y_i are shown in figure 3. The y_{24} value shown in figure 3 is the same as the y_{24} of figure 1 and is not relevant in this table. The x_i dimensions are such that the y axis passes through the center of the active air cavity volume when the Farmer chamber is in place. The x_i values on either side of the y axis are linear dimensions from the y axis. The y_i values are cylindrical radii. Note that the meanings of the x_i and y_i values in this table are the swap of their meanings in table 3; this is because the irradiation is side-on.

i	Dimension in cm		
in x_i	Hevimet	PMMA	Al
Left side of y axis			
17	1.8195	5.4705	2.3205
18	1.2683	1.2683	1.2683
19	1.2271	1.2266	1.2254
Right side of y axis			
20	1.0729	1.0734	1.0746
21	1.2800	1.2800	1.2800
22	1.3005	3.4595	2.5695
23	1.7119	6.1364	4.2135
i	Dimension in cm		
in y_i	Hevimet	PMMA	Al
25	0.3587	0.3579	0.3558
26	0.4300	0.4300	0.4300
27	0.7125	4.6365	2.8475

4 Tabulated results

The measured and the `EGSnrc`-calculated transmission data are given in table 7, and they correspond to the graphical results in figure 8 of the original publication (Ali *et al* 2012). The experimental and the `EGSnrc` sensitivity results are given in table 8, and they correspond to the graphical results in figure 7 of the original publication.

Table 7: Data of figure 8 of the original publication (Ali *et al* 2012). The table provides the experimental transmission data, T_{exp} and the `EGSnrc`-calculated data, T_{EGSnrc}, for different beams, targets and attenuators. The ratio R is defined as T_{EGSnrc}/T_{exp}. All the data in this table are with the Exradin A19 Farmer chamber. The index of the attenuator length, i, corresponds to the first column in table 5. The uncertainty values are one standard uncertainty in per cent, and they are independent of the cap. The total uncertainty on T_{EGSnrc} from the budget in the original publication is 0.25% for all data. The uncertainty, u_{exp}, on T_{exp} includes the components due to electron beam uncertainties since this is a primary benchmark. The uncertainty, u_R, on a ratio, R, is obtained by adding the experimental and the Monte Carlo uncertainties in quadrature. See the original publication for more details. The table continues in the following two pages.

i	T_{exp}	T_{EGSnrc}	R	i	T_{exp}	T_{EGSnrc}	R	u_{exp}	u_R
(a) 10 MV, Al target									
C att., Hevimet cap				C att., PMMA cap					
2	3.716×10^{-1}	3.771×10^{-1}	1.015	1	5.576×10^{-1}	5.595×10^{-1}	1.003	0.47	0.53
4	1.594×10^{-1}	1.615×10^{-1}	1.013	3	2.074×10^{-1}	2.090×10^{-1}	1.008	0.60	0.65
6	7.380×10^{-2}	7.540×10^{-2}	1.022	5	8.604×10^{-2}	8.780×10^{-2}	1.020	0.71	0.75
8	3.364×10^{-2}	3.454×10^{-2}	1.027	7	3.915×10^{-2}	3.989×10^{-2}	1.019	0.80	0.84
10	1.651×10^{-2}	1.706×10^{-2}	1.034	9	1.809×10^{-2}	1.860×10^{-2}	1.028	0.88	0.92
Pb att., Hevimet cap				Pb att., PMMA cap					
2	4.320×10^{-1}	4.315×10^{-1}	0.999	1	6.176×10^{-1}	6.161×10^{-1}	0.998	0.45	0.51
4	1.977×10^{-1}	1.961×10^{-1}	0.992	3	2.728×10^{-1}	2.713×10^{-1}	0.995	0.48	0.55
6	9.173×10^{-2}	9.172×10^{-2}	1.000	5	1.248×10^{-1}	1.242×10^{-1}	0.995	0.52	0.58
8	4.331×10^{-2}	4.308×10^{-2}	0.995	7	5.822×10^{-2}	5.771×10^{-2}	0.991	0.55	0.60
10	2.026×10^{-2}	2.009×10^{-2}	0.991	9	2.740×10^{-2}	2.727×10^{-2}	0.995	0.58	0.63

...continuation of table 7 from the previous page.

i	T_{exp}	T_{EGSnrc}	R	i	T_{exp}	T_{EGSnrc}	R	u_{exp}	u_R
(b) 15 MV, Be target									
C att., Hevimet cap				C att., PMMA cap					
2	4.089×10^{-1}	4.098×10^{-1}	1.002	1	5.834×10^{-1}	5.823×10^{-1}	0.998	0.33	0.41
4	1.845×10^{-1}	1.857×10^{-1}	1.007	3	2.274×10^{-1}	2.272×10^{-1}	0.999	0.43	0.50
6	8.862×10^{-2}	8.940×10^{-2}	1.009	5	9.923×10^{-2}	9.961×10^{-2}	1.004	0.51	0.57
8	4.233×10^{-2}	4.275×10^{-2}	1.010	7	4.579×10^{-2}	4.614×10^{-2}	1.008	0.58	0.63
10	2.123×10^{-2}	2.148×10^{-2}	1.011	9	2.217×10^{-2}	2.244×10^{-2}	1.012	0.64	0.68
Pb att., Hevimet cap				Pb att., PMMA cap					
2	4.338×10^{-1}	4.333×10^{-1}	0.999	1	6.384×10^{-1}	6.364×10^{-1}	0.997	0.31	0.40
4	1.950×10^{-1}	1.940×10^{-1}	0.995	3	2.840×10^{-1}	2.820×10^{-1}	0.993	0.35	0.43
6	8.841×10^{-2}	8.821×10^{-2}	0.998	5	1.287×10^{-1}	1.284×10^{-1}	0.997	0.38	0.46
8	4.067×10^{-2}	4.060×10^{-2}	0.998	7	5.925×10^{-2}	5.886×10^{-2}	0.993	0.41	0.48
10	1.857×10^{-2}	1.850×10^{-2}	0.996	9	2.755×10^{-2}	2.741×10^{-2}	0.995	0.44	0.51
(c) 15 MV, Al target									
C att., Hevimet cap				C att., PMMA cap					
2	4.113×10^{-1}	4.119×10^{-1}	1.002	1	5.844×10^{-1}	5.842×10^{-1}	1.000	0.33	0.41
4	1.868×10^{-1}	1.872×10^{-1}	1.003	3	2.282×10^{-1}	2.289×10^{-1}	1.003	0.43	0.50
6	9.013×10^{-2}	9.032×10^{-2}	1.002	5	9.985×10^{-2}	1.007×10^{-1}	1.008	0.51	0.57
8	4.323×10^{-2}	4.354×10^{-2}	1.007	7	4.623×10^{-2}	4.669×10^{-2}	1.010	0.58	0.63
10	2.178×10^{-2}	2.182×10^{-2}	1.002	9	2.247×10^{-2}	2.279×10^{-2}	1.014	0.64	0.68
Pb att., Hevimet cap				Pb att., PMMA cap					
2	4.333×10^{-1}	4.314×10^{-1}	0.996	1	6.390×10^{-1}	6.372×10^{-1}	0.997	0.31	0.40
4	1.944×10^{-1}	1.931×10^{-1}	0.994	3	2.837×10^{-1}	2.817×10^{-1}	0.993	0.35	0.43
6	8.805×10^{-2}	8.811×10^{-2}	1.001	5	1.286×10^{-1}	1.280×10^{-1}	0.996	0.38	0.46
8	4.041×10^{-2}	4.027×10^{-2}	0.996	7	5.921×10^{-2}	5.881×10^{-2}	0.993	0.41	0.48
10	1.849×10^{-2}	1.838×10^{-2}	0.994	9	2.753×10^{-2}	2.741×10^{-2}	0.996	0.44	0.51
(d) 15 MV, Pb target									
C att., Hevimet cap				C att., PMMA cap					
2	4.107×10^{-1}	4.118×10^{-1}	1.003	1	5.926×10^{-1}	5.932×10^{-1}	1.001	0.33	0.41
4	1.861×10^{-1}	1.880×10^{-1}	1.010	3	2.310×10^{-1}	2.337×10^{-1}	1.011	0.43	0.50
6	8.990×10^{-2}	9.073×10^{-2}	1.009	5	1.013×10^{-1}	1.022×10^{-1}	1.009	0.51	0.57
8	4.331×10^{-2}	4.379×10^{-2}	1.011	7	4.679×10^{-2}	4.737×10^{-2}	1.012	0.58	0.63
10	2.194×10^{-2}	2.211×10^{-2}	1.008	9	2.288×10^{-2}	2.325×10^{-2}	1.016	0.64	0.68
Pb att., Hevimet cap				Pb att., PMMA cap					
2	4.346×10^{-1}	4.349×10^{-1}	1.001	1	6.549×10^{-1}	6.532×10^{-1}	0.997	0.31	0.40
4	1.950×10^{-1}	1.941×10^{-1}	0.995	3	2.915×10^{-1}	2.893×10^{-1}	0.993	0.35	0.43
6	8.835×10^{-2}	8.792×10^{-2}	0.995	5	1.321×10^{-1}	1.317×10^{-1}	0.997	0.38	0.46
8	4.060×10^{-2}	4.044×10^{-2}	0.996	7	6.091×10^{-2}	6.025×10^{-2}	0.989	0.41	0.48
10	1.858×10^{-2}	1.840×10^{-2}	0.990	9	2.837×10^{-2}	2.808×10^{-2}	0.990	0.44	0.51

. . . continuation of table 7 from the previous page.

i	T_{exp}	T_{EGSnrc}	R	i	T_{exp}	T_{EGSnrc}	R	u_{exp}	u_R
(e) 20 MV, Al target									
C att., Hevimet cap				C att., PMMA cap					
2	3.927×10^{-1}	3.943×10^{-1}	1.004	1	5.596×10^{-1}	5.611×10^{-1}	1.003	0.33	0.41
4	1.696×10^{-1}	1.700×10^{-1}	1.002	3	2.088×10^{-1}	2.104×10^{-1}	1.008	0.43	0.50
6	7.794×10^{-2}	7.845×10^{-2}	1.007	5	8.633×10^{-2}	8.743×10^{-2}	1.013	0.51	0.57
8	3.607×10^{-2}	3.635×10^{-2}	1.008	7	3.830×10^{-2}	3.882×10^{-2}	1.013	0.58	0.63
10	1.722×10^{-2}	1.743×10^{-2}	1.012	9	1.737×10^{-2}	1.773×10^{-2}	1.021	0.64	0.68
Pb att., Hevimet cap				Pb att., PMMA cap					
2	4.448×10^{-1}	4.459×10^{-1}	1.003	1	6.557×10^{-1}	6.591×10^{-1}	1.005	0.31	0.40
4	2.028×10^{-1}	2.042×10^{-1}	1.007	3	3.006×10^{-1}	3.020×10^{-1}	1.005	0.35	0.43
6	9.076×10^{-2}	9.097×10^{-2}	1.002	5	1.413×10^{-1}	1.417×10^{-1}	1.003	0.38	0.46
8	4.334×10^{-2}	4.355×10^{-2}	1.005	7	6.717×10^{-2}	6.752×10^{-2}	1.005	0.41	0.48
10	2.036×10^{-2}	2.048×10^{-2}	1.006	9	3.209×10^{-2}	3.230×10^{-2}	1.007	0.44	0.51
(f) 20 MV, Pb target									
C att., Hevimet cap				C att., PMMA cap					
2	3.854×10^{-1}	3.870×10^{-1}	1.004	1	5.591×10^{-1}	5.622×10^{-1}	1.006	0.33	0.41
4	1.646×10^{-1}	1.654×10^{-1}	1.005	3	2.045×10^{-1}	2.066×10^{-1}	1.011	0.43	0.50
6	7.525×10^{-2}	7.599×10^{-2}	1.010	5	8.341×10^{-2}	8.482×10^{-2}	1.017	0.51	0.57
8	3.482×10^{-2}	3.509×10^{-2}	1.008	7	3.684×10^{-2}	3.730×10^{-2}	1.013	0.58	0.63
10	1.658×10^{-2}	1.686×10^{-2}	1.017	9	1.667×10^{-2}	1.700×10^{-2}	1.019	0.64	0.68
Pb att., Hevimet cap				Pb att., PMMA cap					
2	4.474×10^{-1}	4.476×10^{-1}	1.001	1	6.688×10^{-1}	6.714×10^{-1}	1.004	0.31	0.40
4	2.045×10^{-1}	2.053×10^{-1}	1.004	3	3.084×10^{-1}	3.104×10^{-1}	1.007	0.35	0.43
6	9.182×10^{-2}	9.230×10^{-2}	1.005	5	1.454×10^{-1}	1.454×10^{-1}	1.000	0.38	0.46
8	4.402×10^{-2}	4.409×10^{-2}	1.002	7	6.938×10^{-2}	6.966×10^{-2}	1.004	0.41	0.48
10	2.073×10^{-2}	2.090×10^{-2}	1.009	9	3.324×10^{-2}	3.342×10^{-2}	1.006	0.44	0.51
(g) 30 MV, Al target									
C att., Hevimet cap				C att., Al cap					
2	4.467×10^{-1}	4.474×10^{-1}	1.002	1	6.322×10^{-1}	6.302×10^{-1}	0.997	0.33	0.41
4	2.112×10^{-1}	2.119×10^{-1}	1.003	3	2.781×10^{-1}	2.783×10^{-1}	1.001	0.43	0.50
6	1.043×10^{-1}	1.051×10^{-1}	1.008	5	1.309×10^{-1}	1.302×10^{-1}	0.994	0.51	0.57
8	5.147×10^{-2}	5.206×10^{-2}	1.011	7	6.307×10^{-2}	6.323×10^{-2}	1.003	0.58	0.63
10	2.602×10^{-2}	2.639×10^{-2}	1.014	9	3.107×10^{-2}	3.136×10^{-2}	1.009	0.64	0.68
Pb att., Hevimet cap				Pb att., Al cap					
2	4.405×10^{-1}	4.421×10^{-1}	1.004	1	6.664×10^{-1}	6.674×10^{-1}	1.001	0.31	0.40
4	2.006×10^{-1}	2.005×10^{-1}	1.000	3	3.060×10^{-1}	3.074×10^{-1}	1.005	0.35	0.43
6	9.173×10^{-2}	9.254×10^{-2}	1.009	5	1.445×10^{-1}	1.442×10^{-1}	0.998	0.38	0.46
8	4.289×10^{-2}	4.345×10^{-2}	1.013	7	6.774×10^{-2}	6.826×10^{-2}	1.008	0.41	0.48
10	2.033×10^{-2}	2.054×10^{-2}	1.010	9	3.288×10^{-2}	3.298×10^{-2}	1.003	0.44	0.51

Table 8: Data of figure 7 of the original publication (Ali *et al* 2012). The table provides the experimental and the `EGSnrc` results for the sensitivity of transmission data to small changes in: (a) the material of the buildup cap, (b) the Farmer chamber construction details, (c) the bremsstrahlung target, and, (d) the incident electron energy. The index of the attenuator length, i, corresponds to the first column in table 5. T_{exp_den} are the experimental transmission data from the denominator of the ratio investigated. R_{exp} and R_{EGSnrc} are, respectively, the experimental and the `EGSnrc` ratio, R, as defined for each set of data. u_{Rexp} is the one standard uncertainty, in per cent, on the experimental ratio. The u_{Rexp} values are smaller than the uncertainties in the previous table because of the correlation between the two signals for a given ratio. The statistical uncertainty on the `EGSnrc` ratio is 0.15% for all data (other Monte Carlo uncertainty components are irrelevant for this relative comparison). See the original publication for more details. The table continues in the following page.

i	T_{exp_den}	R_{exp}	R_{EGSnrc}	i	T_{exp_den}	R_{exp}	R_{EGSnrc}	u_{Rexp}
(a) $R = T$(Al cap) / T(PMMA cap), 15 MV, C att, A19								
Be target				Pb target				
1	5.834×10^{-1}	1.028	1.025	1	5.926×10^{-1}	1.025	1.023	0.10
3	2.274×10^{-1}	1.066	1.066	3	2.310×10^{-1}	1.061	1.062	0.15
5	9.923×10^{-2}	1.093	1.093	5	1.013×10^{-1}	1.088	1.087	0.18
7	4.579×10^{-2}	1.118	1.110	7	4.679×10^{-2}	1.116	1.117	0.21
9	2.217×10^{-2}	1.128	1.127	9	2.288×10^{-2}	1.135	1.130	0.23
(b) $R = T$(PTW30013) / T(A19), 30 MV, Al target, C att, Hevimet cap								
2	4.467×10^{-1}	0.9961	0.9965					0.07
4	2.112×10^{-1}	0.9942	0.9959					0.11
6	1.043×10^{-1}	0.9931	0.9960					0.14
8	5.147×10^{-2}	0.9922	0.9936					0.16
10	2.602×10^{-2}	0.9905	0.9929					0.18
(c) $R = T$(Pb target) / T(Al target), 20 MV, A19								
C att., Hevimet cap				C att., PMMA cap				
2	3.927×10^{-1}	0.981	0.981	1	5.596×10^{-1}	0.999	1.002	0.10
4	1.696×10^{-1}	0.971	0.973	3	2.088×10^{-1}	0.979	0.982	0.15
6	7.794×10^{-2}	0.966	0.969	5	8.633×10^{-2}	0.966	0.970	0.18
8	3.607×10^{-2}	0.965	0.965	7	3.830×10^{-2}	0.962	0.961	0.21
10	1.722×10^{-2}	0.963	0.967	9	1.737×10^{-2}	0.960	0.959	0.23
Pb att., Hevimet cap				Pb att., PMMA cap				
2	4.448×10^{-1}	1.006	1.004	1	6.557×10^{-1}	1.020	1.019	0.10
4	2.028×10^{-1}	1.008	1.005	3	3.006×10^{-1}	1.026	1.028	0.15
6	9.076×10^{-2}	1.012	1.015	5	1.413×10^{-1}	1.029	1.026	0.18
8	4.334×10^{-2}	1.016	1.012	7	6.717×10^{-2}	1.033	1.032	0.21
10	2.036×10^{-2}	1.018	1.021	9	3.209×10^{-2}	1.036	1.035	0.23

. . . continuation of table 8 from the previous page.

i	T_{exp_den}	R_{exp}	R_{EGSnrc}	i	T_{exp_den}	R_{exp}	R_{EGSnrc}	u_{Rexp}
(d) $R = T$(15.7 MV) / T(15.0 MV), Pb target, A19, Hevimet cap								
C attenuator				Pb attenuator				
2	4.107×10^{-1}	1.016	1.020	2	4.346×10^{-1}	0.996	0.996	0.10
4	1.861×10^{-1}	1.031	1.030	4	1.950×10^{-1}	0.990	0.991	0.15
6	8.990×10^{-2}	1.044	1.046	6	8.835×10^{-2}	0.986	0.991	0.18
8	4.331×10^{-2}	1.060	1.056	8	4.060×10^{-2}	0.984	0.984	0.21
10	2.194×10^{-2}	1.077	1.069	10	1.858×10^{-2}	0.980	0.978	0.23

5 References

Ali E S M, McEwen M R and Rogers D W O 2012 Detailed high-accuracy megavoltage transmission measurements: A sensitive experimental benchmark of EGSnrc *Med. Phys.* tentatively accepted

Kawrakow I 2000 Accurate condensed history Monte Carlo simulation of electron transport. I. EGSnrc, the new EGS4 version *Med. Phys.* **27** 485 – 498

Kawrakow I, Mainegra-Hing E, Rogers D W O, Tessier F and Walters B R B 2011 The EGSnrc Code System: Monte Carlo simulation of electron and photon transport NRC Technical Report PIRS-701 v4-2-3-2, National Research Council Canada, Ottawa, Canada. http://www.irs.inms.nrc.ca/inms/irs/EGSnrc/EGSnrc.html

Muir B R and Rogers D W O 2010 Monte Carlo calculations of k_Q, the beam quality conversion factor *Med. Phys.* **37** 5939 – 5950